Inelastic neutron scattering study on the electronic transition in (Pr_{1−y}Y_{y})_{1−x}Ca_{x}CoO_{3} single crystals

Taketo Moyoshi, Kazuya Kamazawa, Masaaki Matsuda, and Masatoshi Sato

Inelastic neutron scattering study on the electronic state change in $(\mathrm{Pr}_{1-y}\mathrm{Y}_y)_{1-x}\mathrm{Ca}_x\mathrm{CoO}_3$ single crystals

Taketo Moyoshi[1,†], Kazuya Kamazawa[1,§,♯], Masaaki Matsuda[2], and Masatoshi Sato[3,‡]

[1]*Neutron Science and Technology Center, Comprehensive Research Organization for Science and Society (CROSS), Tokai, Ibaraki 319-1106, Japan*
[2]*Neutron Scattering Division, Oak Ridge National Laboratory, Oak Ridge, Tennessee 37831, USA* and
[3]*Graduate School of Science, Nagoya University, Chikusa-ku, Nagoya 464-8602, Japan*
(Dated: October 4, 2018)

The perovskite Co oxides $\mathrm{Pr}_{1-x}\mathrm{Ca}_x\mathrm{CoO}_3$ exhibit at around $x \sim 0.5$ an unusual transition at temperature T_S [Tsubouchi *et al.* Phys. Rev. B **66** 052418 (2002).] with no space group change and no long range magnetic order. We measured inelastic neutron scattering intensities of magnetic excitations $I(\boldsymbol{Q}, \omega)$ for two single crystals of $(\mathrm{Pr}_{1-y}\mathrm{Y}_y)_{1-x}\mathrm{Ca}_x\mathrm{CoO}_3$ in which the x-region of the transition is widened by the Pr-site doping, to study whether the recent proposal of the excitonic condensation model is relevant to this "hidden order transition" of the system. While the $\chi"(\boldsymbol{Q}, \omega)$ seems to have characteristics of strongly correlated Co $3d$ electrons above T_S, it abruptly exhibits a weak feature reminiscent of a pseudogap-like structure at T_S with decreasing T. The first peak of the Pr crystal-field-excitations has also been observed at low temperatures. Here, using a model of the coexistence of the exciton condensed phase (EC phase) with the nearly or weakly ferromagnetic one, we show that the EC phase appears as the collective transition in $\mathrm{Pr}_{1-x}\mathrm{Ca}_x\mathrm{CoO}_3$.

PACS numbers: 71.35.-y, 67.85.Hj, 67.85.Jk, 28.20.Cz,78.70.Nx

I. INTRODUCTION

The $\mathrm{Pr}_{1-x}\mathrm{Ca}_x\mathrm{CoO}_3$ system has the perovskite-type structure with the corner-sharing network of CoO_6 octahedra. In the very narrow region of $x \sim 0.5$, Tsubouchi *et al.* [1] found a new-type first order transition accompanied with the abrupt decrease of the magnetic susceptibility (χ) and rapid increase of the resistivity (ρ) at temperature $T = T_S$ (~ 80 K) with decreasing T. The detailed phase diagram with two other low-T phases, phase I ($x \leq 0.2$; paramagnetic insulating) and phase II ($0.2 \leq x \leq 0.5$-δ; nearly or weakly ferromagnetic metallic) were reported in their second paper [2]. We call here the new-type-phase, phase III ($x \sim 0.5$). To investigate the origin(s) of the transition at T_S, and to identify the ground state of $\mathrm{Pr}_{0.5}\mathrm{Ca}_{0.5}\mathrm{CoO}_3$, $(\mathrm{Pr}_{1-y}\mathrm{Y}_y)_{1-x}\mathrm{Ca}_x\mathrm{CoO}_3$ (R = lanthanides and Y) was adopted to collect effects of the R-atom doping and pressure application on the basic physical quantities and structures [3]-[6]. Tong *et al.* also reported the structure of $\mathrm{Pr}_{0.5}\mathrm{Ca}_{0.5}\mathrm{CoO}_3$ [7]. The notable characteristics of the Pr-based system found by these studies are as follows. (1) $\mathrm{Pr}_{0.5}\mathrm{Ca}_{0.5}\mathrm{CoO}_3$ seemed to have a "hidden order transition" at T_S, that is, the space group ($Pnma$) did not change at the transition and no long-range order was identified down to ~ 10 K ($\ll T_S$). (2) While the anomalous contraction of the unit cell volume is found at T_S, the CoO_6 octahedra expand with decreasing T. (3) The tilting angle of CoO_6 octahedra suddenly increases at T_S together with the χ-decrease and ρ-increase with decreasing T, but none of these quantities exhibits such the anomaly when the system temperature is lowered to the phases I or II. Following facts can also be listed. (4) The transition to the phase III is found only in the Pr containing system $(\mathrm{Pr}_{1-y}\mathrm{R}_y)_{1-x}\mathrm{Ca}_x\mathrm{CoO}_3$. (5) The partial substitution of

Pr with smaller R atoms and/or the application of external pressure (p) significantly expand(s) the x region of this type transition from a very narrow region of $x \sim 0.5$ to the region of much smaller x. (6) An electron transfer from Pr to Co sites was suggested [4][5] by a model [8] used in the arguments on the non-existence of the superconductivity in $\mathrm{PrBa}_2\mathrm{Cu}_3\mathrm{O}_7$. These results suggest that the complicated interplay of various factors has to be considered to thoroughly understand what determines the behavior of the system, the energy difference Δ between the e_g and t_{2g} bands, doped hole number, volume of the unit cell or CoO_6 octahedra, transport nature of the electrons, tilting angle of the octahedra or coupling of the electrons to the lattice system, and so on.

To understand this transition in a microscopic way, the exciton condensation model was proposed [9]-[12] by considering the condensation of atomic size excitons with spin $S = 1$ (triplet). The Pr-valence change was also considered. In the model, the electrons in the upper e_g level remain in the condensed phase, contradicting a model of the [high-spin (HS) or intermediate spin (IS)] $\leftrightarrow$ low-spin (LS) change of a single Co^{3+} site. However, it can explain the experimental data already reported at that time by X-ray absorption near edge structure (XANES) studies [13]-[19]. It is also consistent with the observed expansion of the CoO_6 octahedra below T_S. The considerations of the Pr-valence change seem to have added a new aspect to the studies of the physics of the system, because the electron number of Co atoms is added to the variable parameters to determine the physical behaviors. Many other theoretical works have been published by various models to study the exciton condensed states [20]-[23].

We have carried out inelastic neutron scattering measurements of magnetic scattering intensities $I(\boldsymbol{Q}, \omega)$ at HB-1 of ORNL on two crystals of $(\mathrm{Pr}_{1-y}\mathrm{Y}_y)_{1-x}\mathrm{Ca}_x\mathrm{CoO}_3$
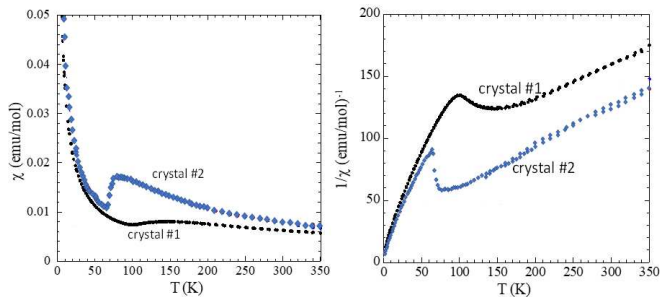
FIG. 1: (color online) (a)The magnetic susceptibilities χ and (b) inverse susceptibility $1/\chi$ are shown against T. They were measured under external magnetic field of 1 T on small pieces from crystals $\sharp1$ and $\sharp2$ of $(\mathrm{Pr}_{1-y}\mathrm{Y}_y)_{0.7}\mathrm{Ca}_{0.3}\mathrm{CoO}_3$.

with the T_S values of ~ 150 K and ~ 80 K, where $\boldsymbol{Q}$ and ω are the scattering vector of the pseudo cubic cell and excitation energy, respectively. Here, we argue the measured data giving information on the curious transition in $(\mathrm{Pr}_{1-y}\mathrm{Y}_y)_{1-x}\mathrm{Ca}_x\mathrm{CoO}_3$.

II. SAMPLES AND EXPERIMENTS

Two single crystals of $(\mathrm{Pr}_{1-y}\mathrm{Y}_y)_{1-x}\mathrm{Ca}_x\mathrm{CoO}_3$ were prepared by the floating zone (FZ) method [24]. Their magnetic susceptibilities χ were measured by using a Quantum Design SQUID magnetometer under magnetic field (H) of 1 T in the temperature range between 2 and 350 K. The data of χ and $1/\chi$ obtained for small pieces from the crystals $\sharp1$ and $\sharp2$ are shown against T in Fig. 1, where the T_S values are found to be ~ 150 K and ~ 80 K, respectively.

Inelastic neutron scattering measurements were carried out using the thermal triple axis spectrometer HB-1 installed at the High Flux Isotope Reactor (HFIR) at Oak Ridge National Laboratory. The horizontal collimations were 48'-80'-80'-240'. The single crystal in an Al can filled with He gas was mounted with the [110] and [001] axes of the pseudo cubic cell within the scattering plane. The scattered neutron energy (E_f) was fixed at 13.5 meV. A PG filter was placed after the sample to eliminate higher order contaminations. In Fig. 2, T dependences of the orthorhombic cell volume (four times larger than the pseudo cubic pervskite cell) deduced from the neutron diffraction data of the crystals $\sharp1$ and $\sharp2$ crystals are shown together with several example data (broken lines) on the powder samples [4][5]. We find that the cell volumes of these crystals exhibit the anomalous contraction with decreasing T at the temperature of the χ-anomaly (T_S), confirming that the Y-doping expands the x region of the "hidden order transition" as is expected from the results for the powder samples [1][4]. The bulk nature of the transition was confirmed by these data. The (x, y) values were roughly estimated to be $(0.3, \sim 0.2)$ and $(0.3, \sim 0.08)$ for the crystals $\sharp1$ and $\sharp2$,
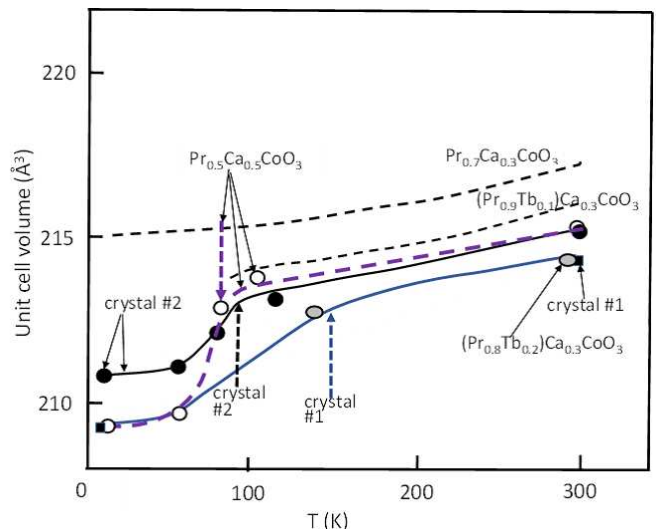
FIG. 2: (color online) The unit cell volumes of the crystals $\sharp1$ and $\sharp2$ obtained by neutron measurements are shown against T together with those reported for the X-ray data of powder samples [4]. The T_S values of the crystals $\sharp1$ and $\sharp2$ and $\mathrm{Pr}_{0.5}\mathrm{Ca}_{0.5}\mathrm{CoO}_3$ powder are indicated by the broken arrows. For other powder samples, no transition was observed down to 4 K. The volume contraction observed for the crystal samples indicates that the transition at T_S is, at least, in a significant volume.

respectively, by comparing the data with those of polycrystalline samples [4][5].

III. RESULTS

We measured the magnetic excitation intensities $I(\boldsymbol{Q}, \omega)$ at several fixed $\boldsymbol{Q}$ points by scanning the excitation energy ω at 4 K and 200 K for the crystal $\sharp1$($T_\mathrm{S} \sim 150$ K), and at 4 K, 30 K, 60 K, 80 K and 120 K for the crystal $\sharp2$ ($T_\mathrm{S} \sim 80$ K). Figure 3 shows the first examples of the spectral functions of the magnetic excitations, $\chi"(\boldsymbol{Q}, \omega) = I(\boldsymbol{Q}, \omega)/(n + 1)$ observed here for the crystal $\sharp1$ at 4 K and 200 K [24] with n being the Bose factor. We consider here that the data at 200 K ($> T_\mathrm{S}$) have a main origin of the correlated 3d electrons, as those of Cu-oxide superconductors in their normal state [25][26] and LaCoO_3 above the temperature of the spin-state crossover[27], although their characteristics depend on their own microscopic parameters determining the transport, magnetic and other physical properties. The spectra at 4 K have an additional sharp Gaussian-like component at ~ 4 meV from the crystal-field excitation (CFE) of Pr ions. Because the broad-energy component seems to have a weak pseudogap-like (concave) in the region of small ω, we try to consider it here as the contribution from the Co electrons and describe its spectral weight as the first term of the right hand side of the following total spectral function. $\chi"(\boldsymbol{Q}, \omega) \propto \hbar\Gamma_{\boldsymbol{Q}}\omega/[\hbar^2(\omega\text{-}$
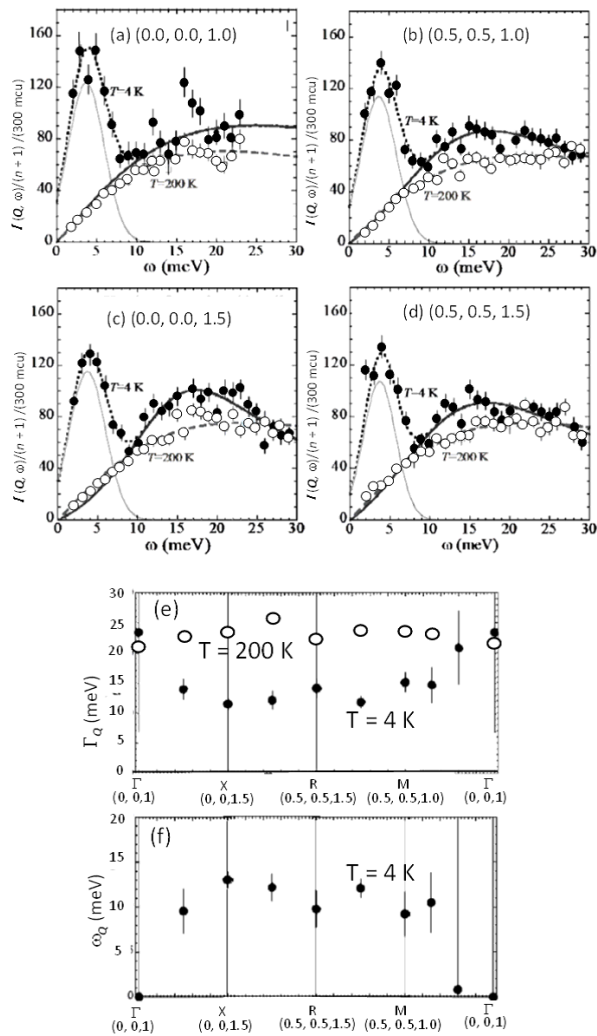
FIG. 3: (color online) [(a) - (d)] Examples of the fittings of *eq.* (1) to the data $\chi''(\boldsymbol{Q}, \omega)$ [$\equiv I(\boldsymbol{Q}, \omega)/(n+1)$] of the crystal $\sharp$1 are shown at four fixed $\boldsymbol{Q}$ points, where the second component of *eq.* (1) cannot be seen at 200 K. $\Gamma_{\boldsymbol{Q}}$ and $\omega_{\boldsymbol{Q}}$ values obtained in the fittings are shown in (e) and (f), respectively. The T and $\boldsymbol{Q}$ values are in the figures. [Note that at 200 K, the error bars of $\Gamma_{\boldsymbol{Q}}$ are smaller than the symbol size and that there are no data points of $\omega_{\boldsymbol{Q}}$ at 200 K, because it is fixed at zero in the fittings.] As shown by the thick dotted lines in (a) - (d), the $\chi''(\boldsymbol{Q}, \omega)$ data at 4 K(solid circles) can be reproduced well by the sum of the two components, one proportional to $\hbar\Gamma_{\boldsymbol{Q}}\omega/[\hbar^2(\omega-\omega_{\boldsymbol{Q}})^2+\Gamma_{\boldsymbol{Q}}^2]$ (thick solid line) and the other contributed by the first CFE of Pr ions (thin solid lines). At 4 K, it is found that the thick solid lines have the pseudogap-like (or concave) nature in the low-ω region. Note that above $\omega \sim 10$ meV, the thick dotted and thick solid lines overlap each other. The $\chi''(\boldsymbol{Q}, \omega)$ data at 200 K (open circles) can be well reproduced at all $\boldsymbol{Q}$ points by the functional form of the first component of *eq.* (1) with the fixed value of $\omega_{\boldsymbol{Q}}$ = 0, indicating that the concave structure does not exist at high T. At 4 K, the $\omega_{\boldsymbol{Q}}$ values seem to approach zero as $\boldsymbol{Q}$ approaches the Γ point, although the error bar is very large. See text for details.

$\omega_{\boldsymbol{Q}})^2+\Gamma_{\boldsymbol{Q}}^2]$ + Gaussian-like component (1), ignoring the additional term $\hbar\Gamma_{\boldsymbol{Q}}\omega/[\hbar^2(\omega+\omega_{\boldsymbol{Q}})^2+\Gamma_{\boldsymbol{Q}}^2]$ [28] required to satisfy the ω-odd condition. This treatment is considered to be approximately correct only with the condition $\Gamma_{\boldsymbol{Q}}^2 \ll \omega_{\boldsymbol{Q}}^2$. However, because even for $\Gamma_{\boldsymbol{Q}}^2 \sim \omega_{\boldsymbol{Q}}^2$, no serious change in the qualitative results are found here by the trial calculations, we use this form below. The second CFE component in *eq.* (1) can be written by using the imaginary part of the single ion susceptibility of Pr ions (basically $\boldsymbol{Q}$ independent), where the Boltzmann statistics is often convenient to treat the crystal field levels of Pr ions. Here, we just used the Gaussian function, because no essential effects are introduced to the results. In the fitting to the ω dependence of $\chi''(\boldsymbol{Q}, \omega)$, the $\omega_{\boldsymbol{Q}}$ and $\Gamma_{\boldsymbol{Q}}$ were treated as the fitting parameters at each fixed $\boldsymbol{Q}$ point. (As only the exception, $\omega_{\boldsymbol{Q}}$ was fixed at zero for crystal $\sharp$1 in the fittings at 200 K.) The width and center energy ω_{cr} of the Gaussian peak were also fitted. No correction of the background counts has been done. We do not consider, for a while, whether the first term in the right hand side of *eq.* (1) contains other CFE's of Pr ions, which may be present with severe broadenings and buried by the observed data in the region higher than the first CFE energy E_1 (~ 4 meV for the crystal $\sharp$1). On this point more detailed arguments are given later.

In Figs. 3(a)-3(d), the $\chi''(\boldsymbol{Q}, \omega)$ observed for the crystal $\sharp$1 at 4 K (solid circles) and 200 K (open circles) are fitted as shown by the thick dotted and gray dashed lines, respectively. All the fittings were carried out to $\chi''(\boldsymbol{Q}, \omega)$ not to the $I(\boldsymbol{Q}, \omega)$ in the ω region studied here [$2.0 \leq \omega \leq 30$ meV]. The thick solid line, which overlaps with the thick dotted lines in the region $\omega \geq 10$ meV, and thin light-gray lines correspond to the $\hbar\Gamma_{\boldsymbol{Q}}\omega/[\hbar^2(\omega-\omega_{\boldsymbol{Q}})^2+\Gamma_{\boldsymbol{Q}}^2]$ term and Gaussian component at 4 K, respectively. At 200 K, the Gaussian term was not observed primarily due to the T dependence of the Boltzmann distribution of the electrons among the crystal field levels. Figures 3(e) and 3(f), the $\Gamma_{\boldsymbol{Q}}$ and $\omega_{\boldsymbol{Q}}$ values obtained in the fittings at the representative points of the Brillouin zone (BZ) of the pseudo cubic perovskite cell with the volume of $\sim a_p^3$. [As stated above, $\omega_{\boldsymbol{Q}}$ was simply fixed at zero in the fittings at 200 K, because the $\chi''(\boldsymbol{Q}, \omega)$ - ω curves have the clear characteristic of $\omega_{\boldsymbol{Q}} \sim 0$, *i.e.*, the gap-like structure cannot be recognized in the first term of *eq.* (1).] Note that the lattice parameters a, b and c of the orthorhombic unit cell can be described as $\sim (2)^{1/2}a_p$, $\sim 2a_p$ and $\sim (2)^{1/2}a_p$, respectively. At 4 K, $\omega_{\boldsymbol{Q}}$ approaches zero as $\boldsymbol{Q}$ approaches the Γ point, though it is not easy to accurately obtain the $\omega_{\boldsymbol{Q}}$ value at the point because of the existence of the strong Gaussian type CEF component. It is also added that by the close inspection of Figs. 3(a)-3(d), we can see at 4K that the $\chi''(\boldsymbol{Q}, \omega)$ - ω curve shows $\boldsymbol{Q}$ dependence, indicating the existence of the contribution of the Co moments. The data supporting this point is described later together with the intensity consideration of the Pr CFE's in the ω region above E_1.

Because the data of the crystal $\sharp$2 seem to have simi-

4(a)

4(b)

4(c)
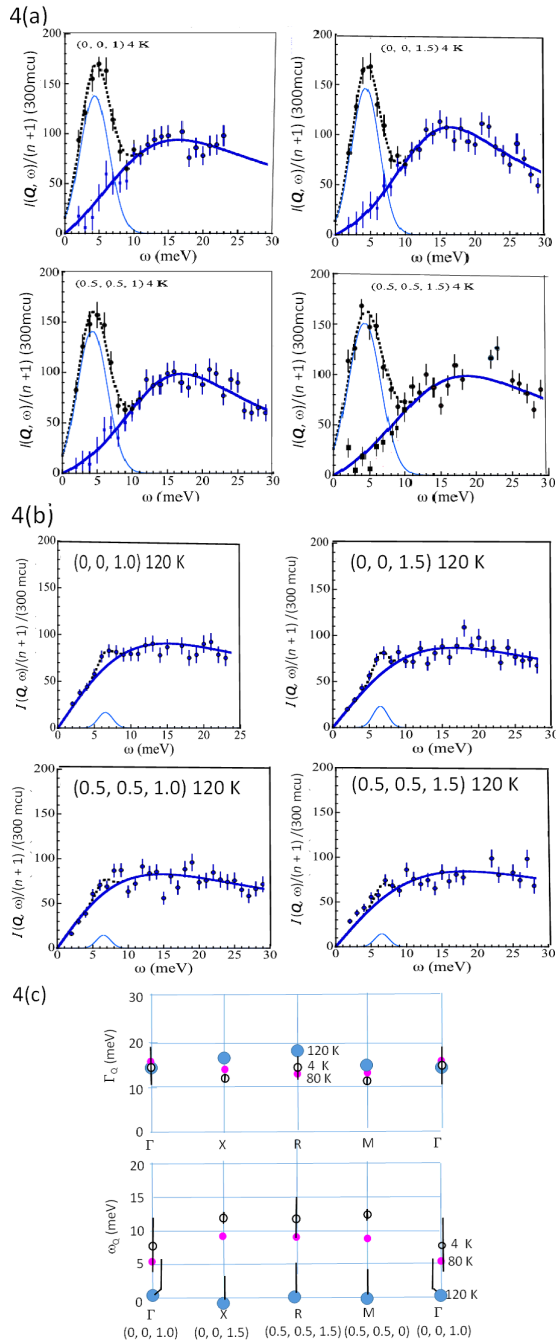
FIG. 4: (color online) (a) Examples of the fittings of *eq.* (1) to the data χ"($\boldsymbol{Q}$, ω) [$\equiv I(\boldsymbol{Q}, \omega)/(n+1)$] at 4 K for the crystal $\sharp$2 are shown at four fixed $\boldsymbol{Q}$ points. The square solid symbols for $\omega \ll 10$ meV show the differences between the observed data and the thin solid line. (b)Eexample of the fittings at 120 K ($> T_S$) are shown for comparison. (c)The $\Gamma_{\boldsymbol{Q}}$ and $\omega_{\boldsymbol{Q}}$ values are shown at 4 K, 80 K and 120 K, with their error bars attached for the selected sets of $\Gamma_{\boldsymbol{Q}}$ or $\omega_{\boldsymbol{Q}}$ and T, where the relatively large values are found for $\omega_{\boldsymbol{Q}}$ at 120 K. Even for the largest error bars, the abrupt change of $\omega_{\boldsymbol{Q}}$ with varying T at around T_S is significant (see Fig. 5, too.).
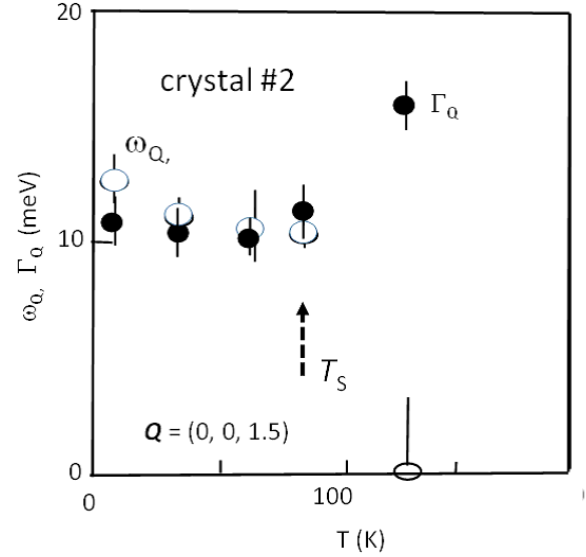
FIG. 5: (color online) The T dependence of the $\omega_{\boldsymbol{Q}}$ and $\Gamma_{\boldsymbol{Q}}$ values at $\boldsymbol{Q} = (0, 0, 1.5)$. At T_S, $\omega_{\boldsymbol{Q}}$ and $\Gamma_{\boldsymbol{Q}}$ exhibit abrupt change, indicating that the concave structures are related to the transition.

lar characteristics to those of the crystal $\sharp$1, the fittings were rather straightforward. The examples of the fittings to the observed χ"($\boldsymbol{Q}$, ω) are shown at four $\boldsymbol{Q}$ values in Figs. 4(a) and 4(b) at 4 K($< T_S$) and at 120 K($> T_S$), respectively, for comparison. Although the clear difference between the characteristics of the χ"($\boldsymbol{Q}$, ω) - ω curves at two temperatures, which supports that $\omega_{\boldsymbol{Q}} \neq 0$ below T_S and $\omega_{\boldsymbol{Q}} \sim 0$ above T_S, $\omega_{\boldsymbol{Q}}$ is included here in the fitting parameters. The $\boldsymbol{Q}$ dependent change of the curves at 4 K can be also found, which is in contrast to the almost $\boldsymbol{Q}$-insensitive behavior of the curves at 120 K. In Fig. 4(c), the $\omega_{\boldsymbol{Q}}$ and $\Gamma_{\boldsymbol{Q}}$ values obtained by the fittings are shown at three temperatures at various $\boldsymbol{Q}$ points in the BZ, where we think that the justification of the relation $\omega_{\boldsymbol{Q}} \sim 0$ is given for the crystals $\sharp$1 and $\sharp$2 above T_S. As compared with the results of crystal $\sharp$1, those of crystal $\sharp$2 seem to have only weak tendencies of the $\omega_{\boldsymbol{Q}}$-decrease and $\Gamma_{\boldsymbol{Q}}$-increase, as $\boldsymbol{Q}$ approaches the Γ point. The T dependences of the $\omega_{\boldsymbol{Q}}$ and $\Gamma_{\boldsymbol{Q}}$ obtained at $\boldsymbol{Q} = (0, 0, 1.5)$ are shown in Fig. 5 as a typical example, where the sudden decrease (increase) of $\omega_{\boldsymbol{Q}}$ ($\Gamma_{\boldsymbol{Q}}$) is found again at T_S with increasing T, indicating that the characteristic change of χ"($\boldsymbol{Q}$, ω) takes place at T_S, even though the pseudogap-like nature of the first term of *eq.* (1) is not so significant (see Fig. 4(a)).

Why is the concave structure weak? One way to answer the question is to consider the first order nature of the transition at T_S and also to consider the other Pr-CFE's in the first term of *eq.* (1), although they are broadened and therefore buried in the Co spin excitations. In the model of the first-order transition,
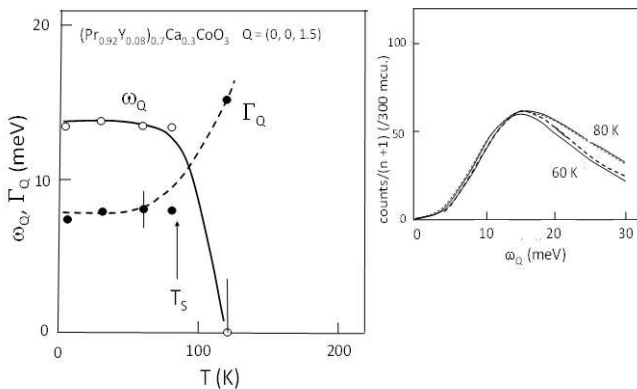
FIG. 6: (color online) T dependences of the ω_Q and Γ_Q values at $Q = (0, 0, 1.5)$ obtained by the model with the two coexisting phases, the EC phase with the volume fraction f and (nearly) ferromagnetic phase below T_S are shown. In this model, the ω_Q and Γ_Q values are larger and smaller than those obtained by the single phase picture of *eq.* (1), respectively. In the right panel, the contributions from the EC phase (solid lines) with the fitted curves (broken lines) are shown.

the nonmagnetic exciton-condensed phase (EC phase) abruptly appears at T_S and coexists in the low-T region with domains or clusters of the nearly or weakly ferromagnetic phase (phase II) [2][4][18]. By this idea, the non-significance of the critical behaviors of $\chi"(Q, \omega)$ at around T_S, or the rather Q and T insensitive behaviors of the observed $\chi"(Q, \omega)$ can be explained, even though the phase II exists adjacent to the phase III below T_S. The sudden changes of the ω_Q and Γ_Q values can be explained, too. As another idea to answer the above question, we presume that the transition to the EC phase (or phase III) does not have effects on $\chi"(Q, \omega)$ so significantly, because the transition is primarily driven by an orbital origin. We make a comment on it in the next section.

The above coexistence model is consistent with the reported results of Phelan *et al* [29]. It is also consistent with the NMR results for $Pr_{0.5}Ca_{0.5}CoO_3$ in Ref. 4, where the abrupt volume-increase of the nonmagnetic phase at T_S with decreasing T and appearance of the internal magnetic field in the zero-field NMR spectra at low temperatures were found. (Note that the NMR measurements cannot often probe the nearly ferromagnetic domains, as is well-known for $La_{1-x}Sr_xCoO_3$ [30].) The theoretical work of Sotnikov and Kunes [12], which considers the Pr valence change has reported that the transition to their polar EC phase becomes the first order-like.

In the actual treatment, we adopt a model for the crystal ♯2 that the first term of *eq.* (1) has two components below T_S, *i.e.*, one from the nonmagnetic parts (EC phase) with the volume fraction f and another with the fraction $(1 - f)$ from the phase II. Above T_S we set $f \sim 0$, and below T_S, f is roughly considered here to be a T independent value, say 0.55, that is, $0.45 \times \chi"(Q, \omega)|_{T=120K}$

is used as the component from the phase II, where $\chi"(Q, \omega)|_{T=120K}$ corresponds to the normal state value of the spectra at 120 K. (Note that 0.45 is the largest value not to have the negative contribution of the nonmagnetic parts in the low-ω region.)
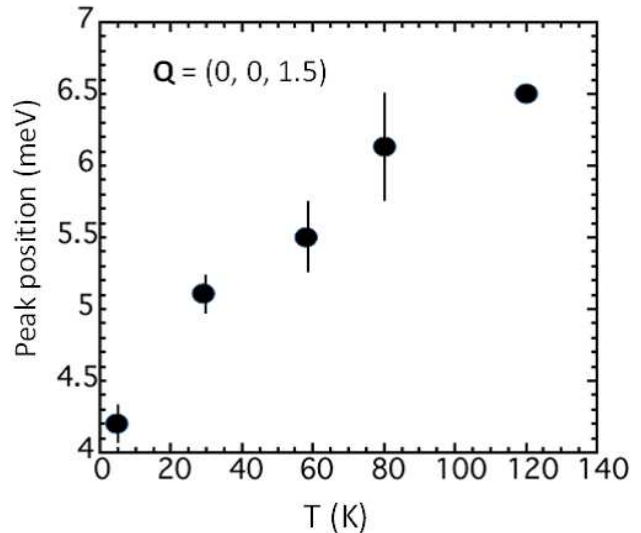
FIG. 7: (color online) The energy positions ω_{cr} at the intensity peak of the observed crystal field excitation are plotted against T.

The contribution of the Pr^{3+}-CFE's buried in the Co excitation is simply included in the $(1 - f)$ fraction, on the basis of the intensity-consideration on the reports for $PrGaO_3$ [31], $PrCoO_3$ [32][33] and $Pr_{1-x}La_xNiO_3$ [34], all of which have the common space group and rather similar crystal field level schemes to those of the present system: Because their integrated intensities can be estimated to have a minor magnitude in the $(1 - f)$ fraction and also because they are sensitive neither T nor electron conductivity, the treatment does not bring about essential changes of the results here, unless the hole doping by the Ca atoms unexpectedly enhances the integrated intensities of these crystal-field excitations (by a factor of ~ 4) relative to the 4 K -values of the first excitation peak at ~ 5 meV. We note here that the intensities of the CFE's of the present crystals are equal to the powder averaged values for powder samples, considering the directions of a, b and c axes of the pseudo cubic systems are equally mixed due to the domain formation.

The ω_Q and Γ_Q at $Q = (0, 0, 1.5)$ thus obtained are shown in Fig. 6 and also the curves fitted to the contribution of the EC phase are in the small right figure, for example, where effects of the transition at T_S on the $\chi"(Q, \omega)$ or on the first term of *eq.* (1) can be found clearer than in Figs. 3 and 4. We stress again the sudden decrease (increase) of $\omega_Q(\Gamma_Q)$ is found at T_S with increasing T, indicating that the characteristic change of $\chi"(Q, \omega)$ takes place at T_S.

In Fig. 7, the peak energies ω_{cr} of the Pr crystal field

excitation observed in Fig. 4 are plotted against T for the crystal ♯2. The ω_{cr} value corresponds to the excitation at the Pr^{3+} sites [15], and its large T dependence may not be related to the Pr valence change.

IV. DISCUSSION

We have analyzed the observed $\chi''(\boldsymbol{Q}, \omega)$ by using the model with the two coexisting phases, where the non-magnetic insulating phase (EC phase of the phase III) appears at T_S in the x region widened by the Y-doping with the significant increase of the resistivity (ρ) and decrease of the dc-magnetic susceptibility (χ) with decreasing T. The sudden increase of the tilting angle of the CoO_6 octahedra found [1][4] at T_S is the evidence for the nonzero coupling between the electrons and lattice system. Therefore, the first order or the abrupt transition is expected, because it can be induced by the interplay among the electrons, lattice and nearly or weakly ferromagnetic clusters. The experiments in ultra-high magnetic field have also revealed the first order nature of the transition [35], although the results do not necessarily indicate the transition is of the first order in the zero field.

As another reason why the critical magnetic behavior is not significant at T_S, we presume that it is because the orbitals have primary roles in the transition [22][23]. Theoretically, Nasu $et~al.$ [22] obtained the excitation spectra for the strong-coupling limit of the two-orbital Hubbard model. Yamaguchi $et~al.$ [23] reported the spin excitation spectra in a five-orbital model using the weak-coupling Hartree-Fock and random phase approximations. In these works, viewpoints of the complicate orbital physics were stressed. However, the idea of the two phase model itself may also be important below T_S as long as the first order nature remains.

Experimentally speaking, we have observed the gap-like or concave feature below T_S, where the T dependences of $\omega_{\boldsymbol{Q}}$ and $\Gamma_{\boldsymbol{Q}}$ shown in Figs. 3 and 4 seem to be rather similar to those reported by Nasu $et~al.$ [22] as one of EC phase, called the EIQ phase. It suggests that the EC phase really exists in the systems, although we cannot experimentally separate the doubly degenerate Goldstone modes and a nondegenerate gapful mode reported in their calculations because of the existence of the strong component of the Pr crystal-field contribution. The EC phase in the phase III is, we think, in the insulating even though the system seems to be macroscopically metallic due to the coexistence with the nearly or weakly ferromagnetic metallic parts.

On the question "which model is realistic as the low-T phase, the EC phase or single-atom LS phase?", our consideration is as follows: Under the external pressure p, the isotropic volume contraction and increase of the electron energy are expected. To release this energy-increase induced by the contraction, the tilting angle of the CoO_6 octahedra suddenly changes at T_S, accompanying the ρ-increase and χ-decrease. We do not know what detailed change occurs for the effective energy difference Δ between the e_g and t_{2g} bands, but know experimentally that ρ is nearly p-independent above T_S and that T_S increases with p [4]. We think that the transition seems to have the collective nature, because the T-width of the resistive transition does not exhibit the meaningful increase with p.

On the other hand, upon the partial substitution for Pr with R atoms smaller than Pr, the volume contraction and χ-decrease also take place at T_S. However, because the distortion induced by the R-atom doping is local, the resistivity above T_S increases with the concentration y, and the T-widths of the ρ and χ anomalies at T_S increase with increasing y [4], indicating that the gradual loss of the collective nature of the transition.

It is worth noting following facts reported previously: (i) T_S of $(Pr_{1-y}Sm_y)_{1-x}Ca_xCoO_3$ shown in Fig. 11 of Ref. 5 has non-monotonic x dependence (or non-monotonic hole-density dependence for fixed y values of 0.2 and 0.3) with a minimum at $x_c \sim 0.3$ and (ii) the smearing or the T-widths of the transition becomes larger with decreasing x below x_c, suggesting that the loss of the collective nature of the anomaly with decreasing x (or with decreasing number of the conducting electrons) induces the change of the nature of the transition. The answer to the question "collective or single atom phenomenon?" seems to depend on various material parameters.

The analysis of $\chi''(\boldsymbol{Q}, \omega)$ with the phase-coexisting model has shown the clear gap-like behavior of the first term of $eq.$ (1). In Figs. 3 and 4, we can find the possible similarity between the experimental results and theoretical calculations [22]. It seems to be the evidence for the existence of the EC phase. However, it is not easy to find other details of the transition. It is desirable to take data on a sample with no disturbance of the doped R atoms and also to take data of the pressure effects on various physical properties, where no irregularity is introduced [4][5].

†deceased
‡Emeritus professor of Nagoya University

§corresponding author
♯k_kamazawa@cross.or.jp

[1] S. Tsubouchi, T. Kyomen, M. Itoh, P. Ganguly, M. Oguni, Y. Shimojo, Y. Morii, and Y. Ishii, Phys. Rev. B **66**, 052418 (2002).

[2] S.Tsubouchi, T. Kyomen, M. Itoh, and M. Oguni, Phys. Rev. B **69** 144406 (2004).

[3] H. Masuda, T. Fujita, T. Miyashita, M. Soda, Y. Yasui, Y. Kobayashi and M. Sato, J. Phys. Soc. Jpn. **72** 873 (2003).

[4] T. Fujita, T. Miyashita, Y. Yasui, Y. Kobayashi, M. Sato, E. Nishibori, M. Sakata, Y. Shimojo, N. Igawa, Y. Ishii, K. Kakurai, T. Adachi, Y. Ohishi and M. Takata, J. Phys. Soc. Jpn. **73**, 1987 (2004).

[5] T. Fujita, S. Kawabata, M. Sato, N. Kurita, M. Hedo and Y. Uwatoko, J. Phys. Soc. Jpn. **74**, 2294 (2005).

[6] T. Naito, H. Sasaki, and H. Fujishiro, J Phys. Soc. Jpn, **79**, 034710 (2010).

[7] P. Tong, Y. Wu, B. Kim, D. Daeyoung, J. M. Sungil Park and B. G. Kim, J. Phys. Soc. Jpn. **78** 034702 (2009).

[8] R. Fehrenbacher and T. M. Rice, Phys. Rev. Lett. **70**, 3471 (1993).

[9] J. Kunes and P. Augustinsky, Phys. Rev. B **89**, 115134 (2014).

[10] J. Kunes and P. Augustinsky, Phys. Rev. B **90**, 235112 (2014).

[11] J. Kunes, Phys. Rev. B **90**, 235140 (2014).

[12] A. Sotnikov and J. Kunes, Phys. Rev. B **96**, 245102 (2017).

[13] Z. Jirák, J. Hejtmánek, K. Knížek, and M. Veverka, Phys. Rev. B **78**, 014432 (2008).

[14] A. J. Barón- González, J. L. García- Muñoz, J. Herrero-Martín, C. Frontera, G. Subías, J. Blasco, and C. Ritter, Phys. Rev. B **81** 054427 (2010).

[15] J. Hejtmánek, E. Šantavá, K. Knížek, M. Maryško, Z. Jirák, T. Naito, H. Sasaki, and H. Fujishiro, Phys. Rev. B **82**, 165107 (2010).

[16] H. Fujishiro, T. Naito, S. Ogawa, N. Yoshida, K. Nittai, J. Hejitmanek, K.Knizek, and Z. Jirak, J. Phys. Soc. Jpn. **81**, 064709 (2012).

[17] J. Herrero-Martín, J. L. García-Muñoz, K. Kvashnina, E. Gallo, G. Subías, J. A. Alonso, and A. J. Barón-González, Phys. Rev. B **86**, 125106 (2012).

[18] J. Hejtmaánek, Z. Jirák, O. Kaman, K. Kníãek, E. San-tava, K. Nitta, T.Naito, and H. Fujishiro, Euro. Phys. J. B **86**, 305 (2013).

[19] H. Fujishiro, T. Naito, D. Takeda, N. Yoshida, T. Watanabe, K. Nitta, J. Hejtmaánek, K. Kníãek, and Z. Jirák, Phys. Rev. B **87**, 155133 (2013).

[20] J. Kunes, Phys. Rev. B **90**, 235140 (2014).

[21] J. Kunes, J. Phys. Condens. Mater., **27**, 333201 (2015).

[22] J. Nasu, T. Watanabe, M. Naka, and S. Ishihara, Phys. Rev. B **93**, 205136 (2016).

[23] T. Yamaguchi, K. Sugimoto, and Yukinori Ohta. J. Phys. Soc. Jpn. **86**, 043701 (2017).

[24] T. Moyoshi, K. Kamazawa, M. Matsuda and M. Sato., Proc. Int. Conf. Neutron Scattering Physica B Available online 23, Nov. 2017, https:/doi.org/10.1016/j.physb.2017.11.055).

[25] J. Rossat-Mignod, L. P. Regnault, C. Vettier, P. Bourges, P. Burlet, J. Bossey, J. Y. Henry and G. Larpertot, Physica C **185-189**, 86-92 (1991).

[26] D. S. Inosov, J. T. Park, P. Bourges, D. L. Sun, Y. Sidis, A. Schneidewind, K. Haradil, D. Haug, C. T. Lin, B. Keimer and V. Hinkov, Nature Physics **6**, 178 (2010).

[27] Y. Kobayashi, T. S. Naing, M. Suzuki, M. Akimitsu, K. Asai, K. Yamada, J. Akimitsu, P. Manuel, J. M. Tranquada and G. Shirane, Phys. Rev. B **72**, 174405 (2005).

[28] J. M. Tranquada, W. J. L. Buyers, H. Chou, T. E. Mason, M. Sao, S. Shamoto and G. Shirane, Phys. Rev. Lett. **64** 800 (1990).

[29] D. Phelan, K. P. Bhatti, M. Taylor, S. Wang, and C. Leighton, Phys. Rev. B **89**, 184427 (2014).

[30] M. Itoh and I. Natori, J. Phys. Soc. Jpn. **64**, 970 (1995).

[31] A. Podlesnyak *etal.*, J. Phys. C **6**, 4099 (1994).

[32] P. Novak, K. Knizek, M. Marysko, Z. Zirak and J. Kunes, J. Phys. Condens. Mater. **25**, 446001 (2013).

[33] Yu, D. Phelan and D. Louca, Phys. Rev. **84** 132410 (2011).

[34] S. Rosenkranz, M. Mandade, F. Fauth, I. Mesot, M. Sollikar, A. Furre, U. Staub, P. Laccore, R. Osborn, R. S. Eccleston and T. Trounov, Phys. Rev. **60**, 14857 (1999).

[35] A. Ikeda, S. Lee, T. T. Terashima, Y. H. Matsuda, M. Tokunaga, and T. Naito, Phys. Rev. B **94**, 115129 (2016).